Supplementary Material: Collaborative Learning of Semi-Supervised Segmentation and Classification for Medical Images

Yi Zhou, Xiaodong He, Lei Huang, Li Liu, Fan Zhu, Shanshan Cui and Ling Shao
Inception Institute of Artificial Intelligence (IIAI), Abu Dhabi, UAE
{yi.zhou, xiaodong.he, lei.huang, li.liu, fan.zhu, shanshan.cui, ling.shao}@inceptioniai.org

1. Data Pre-processing for Fundus Images

Since the fundus images from different datasets have various illuminations and resolutions, we proposed a data pre-processing method extended from [43] (Ref. in the original paper) to unify the image quality and also sharpen the texture details. To keep small lesion areas clear in the images, we set the input image size to 640×640. First, illumination equalization is conducted to balance the brightness of the center of the fundus and the edges of the fundus. By compensating the brightness of the image edge area, the brightness difference between the image edge area and the image center area is minimized. Weighted pixel values are computed based on the distances between the coordinates of the fundus center and each pixel of the fundus image. The brightness after equalization is equal to the brightness of the original image plus the coefficient multiplied by weighted pixel values. The coefficient is calculated by fitting. Moreover, gaussian blur is used to extract low-frequency information in the image, which is reduced by half from the original image to make the high-frequency information (including blood vessel, the edge of the lesion area, etc.) more prominent. The parameter σ of gaussian kernel is equal to 40 divided by the radius of the image. All the images are padded into square for keeping the effective area in the center of the image. Examples of the pre-processed images are shown in the second column in Fig. 1,2,3.

2. Additional Results

2.1. Qualitative Multi-Lesion Segmentation Results on the EyePACS Dataset

To better demonstrate the lesion segmentation performance, Fig. 1,2,3 show more results by our semi-supervised model, including hard exudates, soft exudates, haemorrhages and microaneurysms, on the EyePACS dataset which does not have pixel-level annotations. Qualitatively evaluated by our collaborative domain experts, the segmentation results are very promising on this dataset where the model is trained without pixel-level annotations.

2.2. Patch-based Discriminator for Segmentation

Since the lesion regions in medical images are usually highly small, we keep the input size of the fundus images for our model as large as 640×640. To explore whether the discriminator is good to distinguish holistic large-resolution images and masks, we compared the image-based discriminator to a patch-based one where the receptive field is set to patch. In this baseline, the dense connection in the discriminator is replaced by 1×1 convolution. The discrimination is performed on the 20×20 map. Table. 1 shows the comparison results on the IDRID dataset. The patch-based discriminator gets lower AUC values for the ROC and PR curves than those by the image-based one.

Table 1. Comparisons of image-level and patch-level discriminator for segmentation on the IDRID dataset.

	AUC_ROC		AUC_PR	
Methods	Image	Patch	Image	Patch
Microaneurysms	0.9828	0.9789	0.4960	0.4935
Haemorrhages	0.9779	0.9741	0.6936	0.6891
Hard Exudates	0.9935	0.9903	0.8872	0.8826
Soft Exudates	0.9936	0.9872	0.7407	0.7379

2.3. Confusion Matrix for DR Grading.

To make the effectiveness of our lesion attention model more convincing, we illustrate the confusion matrix of DR grading results on the EyePACS dataset which has a large amount of images. We compared our model to the baseline '**Ori**' without the attention learning in Table. 2. It shows that our model achieves better results on images with high grading levels benefited from lesion segmentation.

Table 2. Confusion matrix for DR grading. L and P denote the ground-truth and predicted labels, respectively. The left value is by our model and the right one is by the baseline.

L \ P	0	1	2	3	4
0	37727/37757	552/1482	1081/163	55/102	119/29
1	1297/1830	1837/1404	603/514	12/9	13/5
2	420/1360	639/664	6144/5009	583/691	75/137
3	18/49	4/16	96/180	1053/847	43/122
4	29/78	3/21	47/191	83/170	1039/747

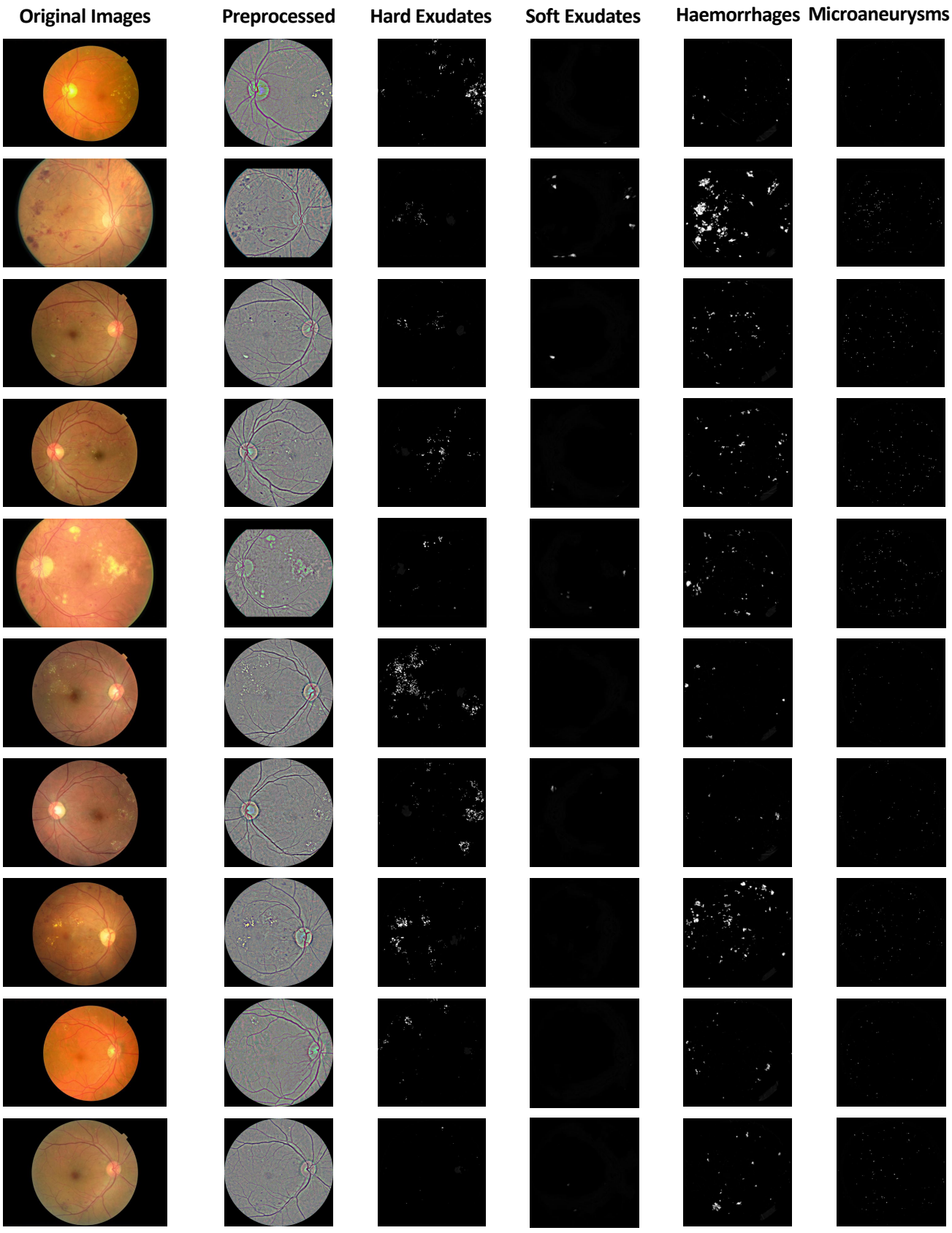

Figure 1. Qualitative multi-lesion segmentation results on the EyePACS dataset. (Best viewed zoomed in.)

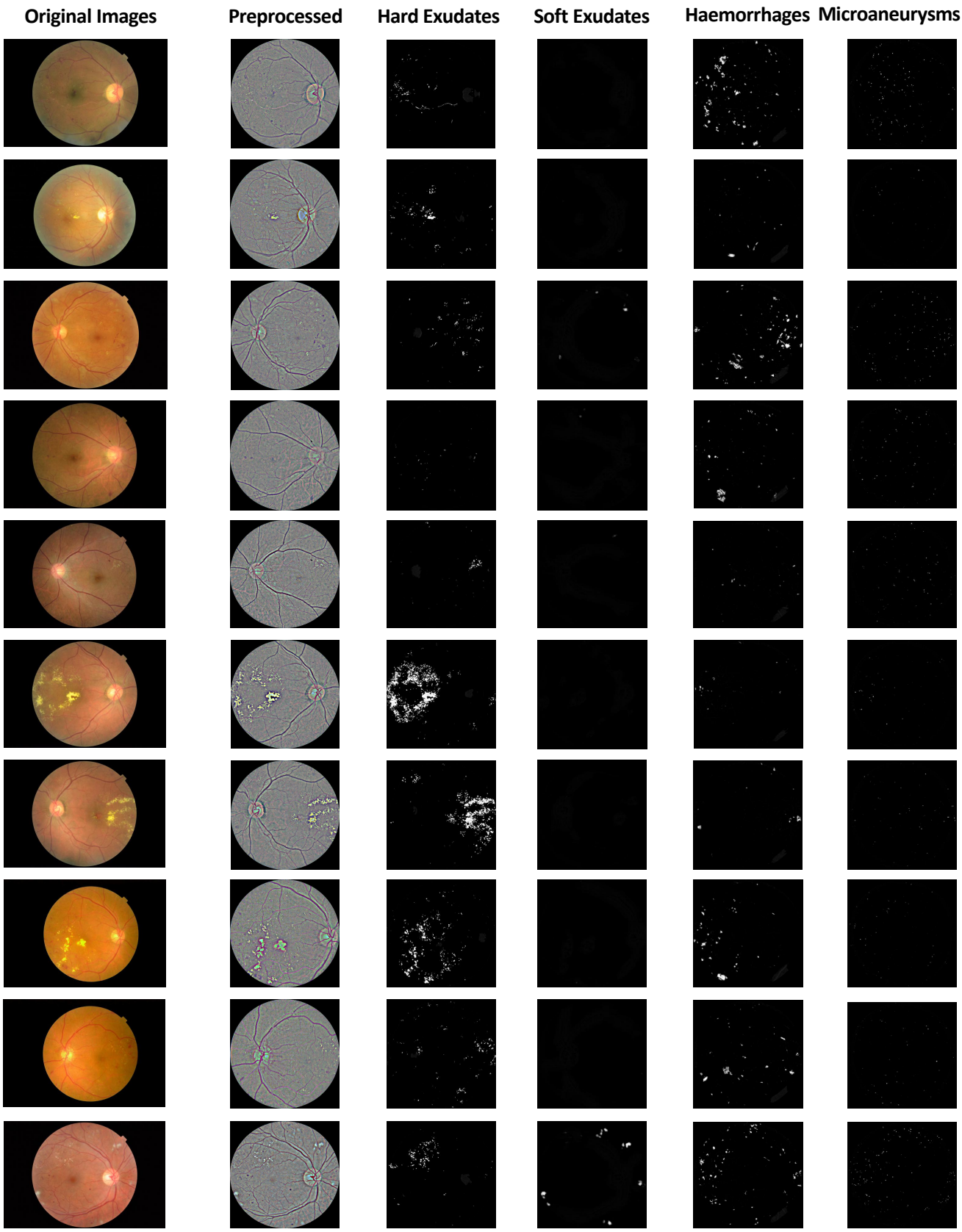

Figure 2. Qualitative multi-lesion segmentation results on the EyePACS dataset. (Best viewed zoomed in.)

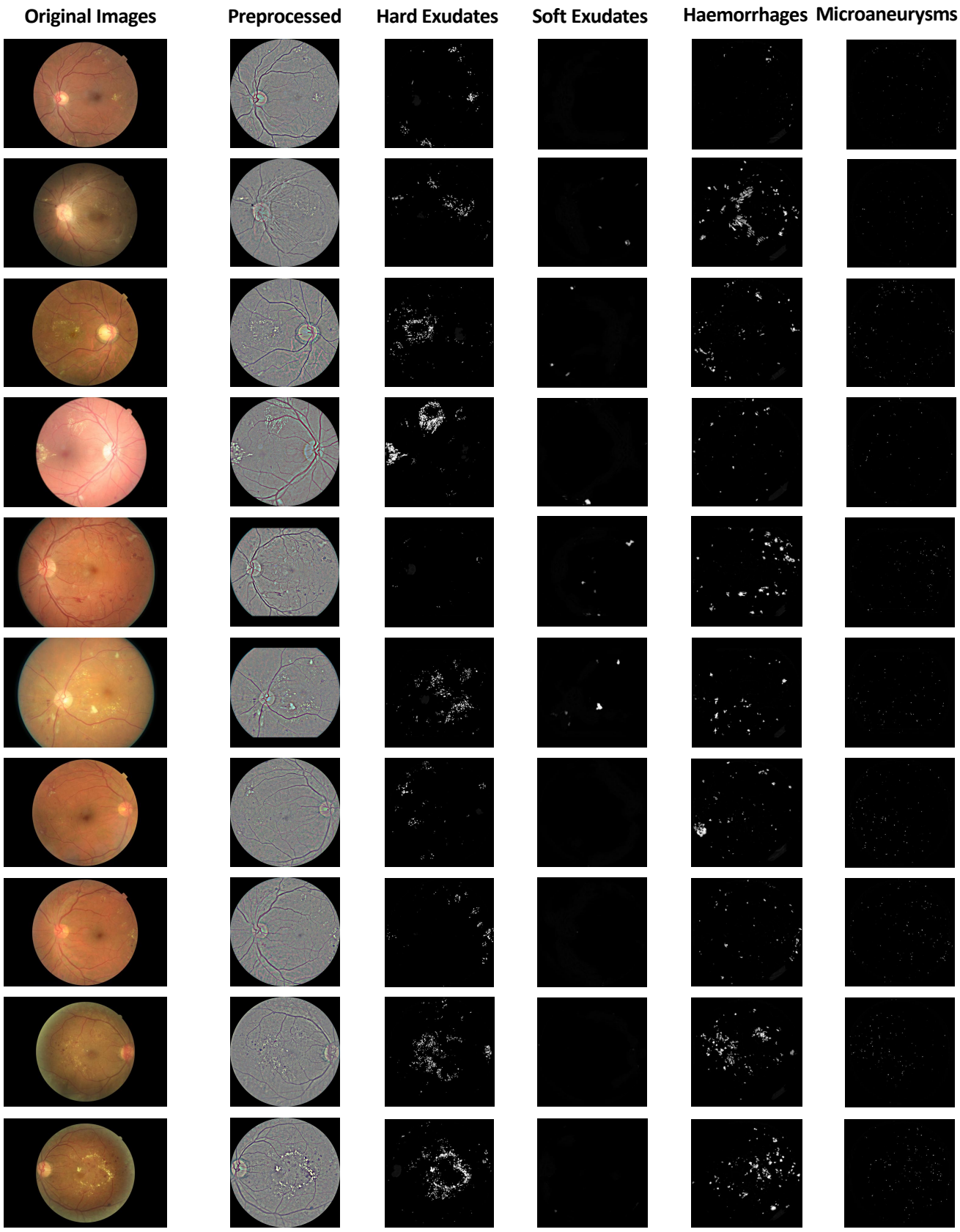

Figure 3. Qualitative multi-lesion segmentation results on the EyePACS dataset. (Best viewed zoomed in.)